Journal Name

ARTICLE

Combining single source chemical vapour deposition precursors to explore the phase space of titanium oxynitride thin films

Received 00th January 20xx,
Accepted 00th January 20xx

DOI: 10.1039/x0xx00000x

www.rsc.org/

Kelly Rees,[a] Emanuela Lorusso,[a] Samuel D. Cosham[a] Alexander N. Kulak[b] and Geoffrey Hyett[a] †

In this paper we report on a novel chemical vapour deposition approach to the formation and control of composition of mixed anion materials, as applied to titanium oxynitride thin films. The method used is the aerosol assisted chemical vapour deposition (AACVD) of a mixture of single source precursors. To explore the titanium-oxygen-nitrogen system the single source precursors selected were tetrakis(dimethylamido) titanium and titanium tetraisopropoxide which individually are precursors to thin films of titanium nitride and titanium dioxide respectively. However, by combining these precursors in specific ratios in a series of AACVD reactions at 400 °C, we are able to deposit thin films of titanium oxynitride with three different structure types and a wide range of compositions. Using this precursor system we can observe films of nitrogen doped *anatase*, with 25% anion doping of nitrogen; a new composition of *pseudobrookite* titanium oxynitride with a composition of $Ti_3O_{3.5}N_{1.5}$, identified as being a UV photocatalyst; and *rock-salt* titanium oxynitride in the range $TiO_{0.41}N_{0.59}$ to $TiO_{0.05}N_{0.95}$. The films were characterised using GIXRD, WDX and UV-vis spectroscopy, and in the case of the pseudobrookite films, assessed for photocatalytic activity. This work shows that a so-called dual single-source CVD approach is an effective method for the deposition of ternary mixed anion ceramic films through simple control of the ratio of the precursors, while keeping all other experimental parameters constant.

Introduction

There is significant interest in mixed anion ceramics, including oxynitrides, oxysulfides and oxyarsenide compounds due to their range of useful properties such as visible light photocatalysis, p-type conductivity and superconductivity.[1-3] For many applications, however, the synthesis of the mixed anion material as a thin film would be desirable. Chemical vapour deposition (CVD) is a widely used and scalable technique for thin film growth,[4-7] and can be used to deposit films of oxides, sulfides, nitrides and indeed mixed anion materials.[4,8-10] However, compared to simple binary phases, mixed anion materials present a significantly greater challenge as their ternary phase diagrams can contain multiple stable structural phases with different anion ratios. It is essential that the deposition route can allow for selective formation of a specific, desired composition.

In this paper we report on a novel method to allow for the controlled deposition of a mixed anion film, and use it to explore the Ti-O-N phase space as a case study. The proposed route makes use of aerosol assisted chemical vapour deposition (AACVD) from a solution of two precursors, tetrakis(dimethylamido) titanium (TDMAT) and titanium tetraisopropoxide (TTIP), which are single source precursors to titanium nitride and titanium dioxide respectively.[11, 12] Our hypothesis is that through the use of these two precursors in an inert solvent - one which cannot act as either nitrogen or oxygen source - it should be possible to control the composition of the deposited film through selection of the ratio of the two precursors, as shown in idealised form in Equation 1. The use of the precursor solution combined with AACVD allows the quantity of the two precursors to be accurately measured and maintained throughout the reaction as they are supplied to the reactor in the same aerosol droplets.

$$x\ Ti(NMe_2)_4 + y\ Ti(O^iPr)_4 \rightarrow (x+y)\ TiO_yN_x + (\text{Organic By-products})$$

Equation 1

The titanium-oxygen-nitrogen system was selected for this work not only because of the diversity of compositions available - it contains at least three distinct structural regions: *anatase*, *rock-salt* and *pseudobrookite*,[13,14] - but also because of the functional nature of these materials as thin films. Titanium dioxide is one of the most widely studied UV activated photocatalysts,[15] and nitrogen doping of titania allows absorption of visible light, increasing the energy available for photocatalysis.[16-18] The *pseudobrookite* structured $Ti_{3-\delta}O_4N$ is also a UV light activated photocatalyst,[19] and the

[a] Department of Chemistry, University of Southampton, Southampton, SO17 1BJ, UK.
[b] School of Chemistry, University of Leeds, Leeds, LS2 9JT, UK
† Corresponding Author: g.hyett@soton.ac.uk

Electronic Supplementary Information (ESI) available: Figure S1 provides a photograph and description of the reactor. Figure S2-S10 are transmission spectra of the samples, and S11 provides data from the visible light photocatalysis study. S12-14 provide SEM images. See DOI: 10.1039/x0xx00000x

Please do not adjust margins

predicted, but as yet to be synthesized more nitrogen rich structural congener $Ti_3O_3N_2$ has also been highlighted as a potential visible light photocatalyst.[20] Finally the *rock-salt* titanium oxynitrides have potential as heat mirrors and in anti-reflection coatings.[21]

Previously reported methods for synthesis of titanium oxynitrides make use of ternary precursor systems, one for each element. For example, atmospheric pressure CVD has been used for synthesis of nitrogen doped *anatase* using titanium tetrachloride, ethyl acetate and butylamine as titanium, oxygen and nitrogen precursors respectively.[22] Replacement of butylamine with ammonia allows the formation of *pseudobrookite* and *rock-salt* titanium oxynitride films.[14] Alternatively, titanium dioxide films can be converted to nitrogen doped titania though post treatment, for example with liquid ammonia followed by annealing.[23] A dual source CVD route to nitrogen doped titania has also been reported using TTIP and hydrazine.[13] However, so far no single precursor system has allowed for controlled deposition of all three phases.

The phase space of titanium-oxygen-nitrogen

A portion of the ternary phase space of the Ti-O-N ceramic system is shown in Figure 1, highlighting the region where titanium is found in the +2 to +4 oxidation state. Compounds with oxidation states below +2 are better characterised as alloys of metallic titanium with oxygen or nitrogen interstitials rather than as ceramic phases.

Along the binary titanium-oxygen line in Figure 1 the most oxygen rich phase is TiO_2 with titanium in its maximum oxidation state. More reduced titanium oxides are known, with the Magneli series Ti_nO_{2n-1} known for n = 2 to 9,[24] culminating in *corundum* structured Ti_2O_3.[25] At lower oxidation states the *rock-salt* structure is found with formal composition TiO. However, this polymorph has a rich defect chemistry, with vacancies on both metal and anion sites, so that a formulation of Ti_xO_y is more appropriate.[26] Some 21 compositions are reported in the *Inorganic Crystal Structure Database* (ICSD) ranging from $TiO_{0.715}$ to $Ti_{0.75}O$,[27,28] with lattice parameters varying between 4.197 Å and 4.161 Å. The presence of defects on both cation and anion sites means that the relationship to composition and unit cell size is complex, however for the *rock-salt* titanium oxides there is a good correlation between the titanium oxidation state and lattice parameter.

For titanium nitrides with a titanium oxidation state greater than +2, the only reported structure is *rock-salt*, although Ti_2N with both *anti-rutile* and *anti-anatase* structures have also been reported in the titanium rich area of the phase diagram not shown in Figure 1.[29,30] The *rock-salt* titanium nitrides, similar to the oxides, have a range of compositions with defects on both metal and anion sites covering a reported range of $Ti_{0.76}N$ to $TiN_{0.9}$.[31,32] The *rock-salt* nitrides have a much smaller lattice parameter range, when compared with the rock salt titanium oxides, of 4.235 Å to 4.245 Å, and there is no clear trend within this range between lattice parameter and titanium oxidation state. A simple ionic argument can explain

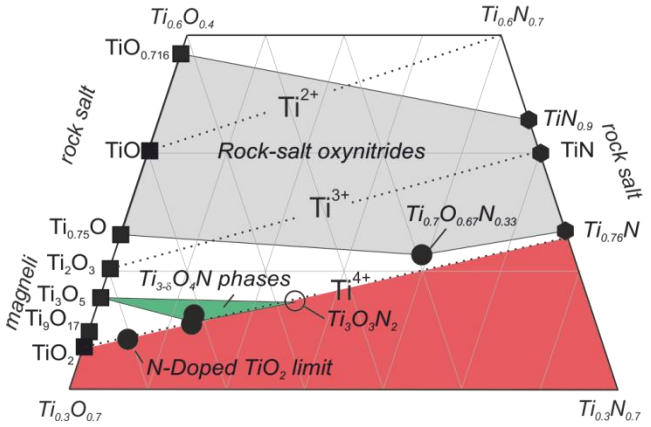

Figure 1. Phase diagram of titanium-oxygen-nitrogen system. Filled shapes represent reported structures, square for oxides, circles for oxynitrides and hexagons for nitrides. The empty circle represents a predicted oxynitride, $Ti_3O_3N_2$. Grey shaded area where *rock-salt* expected, green where *pseudobrookite*.

this. The larger nitride ion provides a close packed lattice which can easily accommodate the relatively small titanium ions (0.67 Å to 0.61 Å for Ti^{3+} to Ti^{4+}), whereas the much smaller close packed lattice of the monoxide has to expand to accept the larger Ti^{2+} ion (0.86 Å). Thus the lattice parameter is more dependent on the titanium oxidation state for the titanium oxides than the titanium nitrides.[33]

The ternary phase space of the titanium oxynitrides is also dominated by the *rock-salt* structure, a solid solution between TiO and TiN which - like the equivalent binary structures - also has a rich defect chemistry such that a broad range of compositions, $Ti_xO_yN_z$, is possible. This is highlighted in Figure 1 by the large central grey section. In addition to the *rock-salt* structure, there is a small range of titanium oxynitrides consisting of what is typically described as 'nitrogen doped TiO_2' adopting the *anatase* structure. This is found to have interstitial or substitutional incorporation of nitrogen, at up to 5 mol%.[34] The final reported titanium oxynitride adopts the *pseudobrookite* structure in the space group *Cmcm* with composition $Ti_{3-\delta}O_4N$ where δ is found between 0.06 to 0.25. These phases are more nitrogen rich than the nitrogen doped *anatase* structures, but unlike the *rock-salt* oxynitrides, titanium in the *pseudobrookite* structures is found close to its maximum oxidation state. The reported *pseudobrookite* titanium oxynitride is structurally related to the Magneli oxide Ti_3O_5 and also to $Ti_3O_3N_2$, the latter more nitrogen rich oxynitride having been predicted by computational modelling to be stable, but not yet observed.[20] The observation of $Ti_{3-\delta}O_4N$ and prediction of $Ti_3O_3N_2$ suggests that there is a small range of *pseudobrookite* structured titanium oxynitrides, $Ti_{3-\delta}O_{5-x}N_x$, with *x* up to 2 which should be stable, and this predicted phase space is highlighted by the green region in Figure 1.

Table 1. Details of the synthetic conditions and results of nine thin film depositions carried out using AACVD at 400°C. [a]The reference name assigned to the film based on fraction of TDMAT precursor used. [b]Volume of the 0.1 M stock TTIP and TDMAT solution added to 8 ml of toluene to make up the precursor solution for each reaction. [c]The lattice parameters of the principle phase identified in each film, as determined by Rietveld refinement. [d]Particle size determined using Scherrer analysis of X-ray peak broadening. [e]Film thickness, determined from side-on SEM images. **Pseudobrookite*

Film Reference[a]	Vol. 0.1 M / ml[b]		Film Colour	Ti/N Ratio	Principal Phase	Lattice Parameters[c]			Particle Size[d] / nm	Thickness[e] / nm
	TTIP	TDMAT				*a* / Å	*b* / Å	*c* / Å		
50%TDMAT	2.00	2.00	Colourless	0.44(3)	*Anatase*	3.772(1)	-	9.448(3)	35	102
60%TDMAT	1.46	2.22	Colourless	0.46(3)	*Anatase*	3.770(1)	-	9.487(3)	32	154
64%TDMAT	1.45	2.55	Colourless	0.48(3)	*Anatase*	3.775(1)	-	9.503(2)	46	199
67%TDMAT	1.33	2.67	Blue	0.50(3)	*PB**	3.759(1)	9.668(2)	9.908(3)	37	314
69%TDMAT	1.33	2.97	Blue	0.52(4)	*PB**	3.752(1)	9.632(5)	9.903(6)	30	301
72%TDMAT	1.14	2.86	Blue	0.59(3)	*Rock-salt*	4.13(1)	-	-	6.2	384
75%TDMAT	1.00	3.00	Blue	0.89(4)	*Rock-salt*	4.15(1)	-	-	10	391
83%TDMAT	0.07	3.33	Blue	0.99(4)	*Rock-salt*	4.19(1)	-	-	8.6	827
100%TDMAT	0.00	4.00	Blue-black	0.95(4)	*Rock-salt*	4.20(1)	-	-	5.3	1000

Experimental Methods

Thin Film Synthesis

Films were deposited by AACVD using a cold-wall reactor. This consisted of a silica tube (58 mm diameter, 170 mm length) with a semi-circular section carbon block insert as a substrate support, itself containing a 745 W cartridge heater (Watlow *Firerod*), as the primary heat source. Two thermocouples were also embedded in the carbon block either side of the cartridge heater to monitor the temperature, and the values measured by these thermocouples provide the deposition temperature reported in this work. The substrates used were silica coated float glass of dimensions 45 × 150 × 3.2 mm^3 (Pilkington NSG). A float glass top-plate was suspended 8 mm above the substrate in order to direct precursor laden carrier gas flow across the substrate.

The precursor solution was held in a 100 ml three necked round bottom flask, partially submerged in a water-filled 600 ml crystallising dish containing a piezoelectric humidifier (Maplin, product no. L38AK). When the flask was positioned above the humidifier it generated a mist of the precursor solution which was transported using a flow of argon gas, controlled by a rotameter, to the reactor. The reactor exhaust was passed through a silicone oil bubbler to prevent back diffusion of air into the reactor. Further details of this reactor are provided in the Supporting Information.

Thin films were deposited using titanium (IV) isopropoxide (TTIP, Sigma Aldrich 99.999%) and tetrakis(dimethylamido) titanium (TDMAT, Sigma Aldrich 99.999%) as precursors dissolved in toluene. TTIP and TDMAT were used as provided, however toluene was dried and degassed prior to use and stored under Argon in a Young's ampoule over 4 Å molecular sieves. Both TTIP and TDMAT were initially made up into separate stock solutions of 0.1 M in toluene. All solutions were prepared and handled using standard Schlenk line techniques. The final precursor solution was made up by dilution in a further 8 ml of toluene and dispensing appropriate volumes of the alkoxide and amide solutions using a Fisherbrand Elite 0.5-5 ml single-channel auto-pipette (0.01 ml resolution). The amount of the individual precursors used varied depending on the reaction, as detailed in Table 1. Reactions were carried out with a carrier gas flow of 1.2 L min^{-1} of argon (BOC, Pureshield) and with a deposition temperature of 400 °C, with each reaction taking 25 to 30 mins for complete transfer of the precursor solution.

Characterisation

X-ray diffraction. Grazing incidence X-ray diffraction patterns were collected from the films using a Rigaku Smart Lab diffractometer equipped with a rotating anode X-ray source (45 kV, 200 mA) in the range 15° < 2θ < 70° and an incident angle of 1°, optimised to maximise diffraction from the film and prevent penetration into the substrate.

SEM/WDX/EDX. A Phillips XL30 environmental scanning electron microscope equipped with an integrated EDS system was used to carry out energy dispersive X-ray analysis with an accelerating voltage of 10 keV. This instrument was also equipped with a Thermofisher MagnaRay WDS which was used to carry out wavelength dispersive X-ray analysis to more accurately quantify the titanium and nitrogen present in each film. Imaging SEM was carried out on a FEI Nova 450 FEG-SEM operating at 5 kV and a working distance of 5 mm.

Spectroscopy. Transmission spectra were collected in the range 200 to 2500 nm using a Lambda 750S spectrometer (Perkin Elmer) equipped with a 100 mm integrating sphere.

Photocatalysis. The photocatalytic ability of the *pseudobrookite* titanium oxynitride films was tested using reduction of an indicator ink, dichloroindophenol (DCIP). In the presence of an activated photocatalyst and a sacrificial

reductant (glycerol) this blue ink undergoes a two electron reduction to a colourless form, and this transformation can be easily monitored using spectroscopy.[35] The test was conducted by placing a section of a film of interest in an 80 ml crystallising dish modified with a water cooling jacket, and adding 25 ml of 1.25×10^{-2} M glycerol and 5.96×10^{-5} M DCIP solution. The sample and dye solution was sealed with a loose fitting lid and allowed to reach equilibrium for 60 mins in the dark before the light was switched on. Aliquots of 3.5 ml of the solution were removed every 30 mins, the absorption spectrum recorded in the range of 400-800 nm, and then returned to the test solution to maintain overall volume. Each test was repeated twice, the first with a LOT-Oriel solar simulator with a measured light intensity at the sample of 509 $mWcm^{-2}$, then using a 365 nm UV light source (CIF, supplied by RS) with an intensity of 4.0 $mWcm^{-2}$. Uncoated glass was also tested as a control.

Results and Discussion

Nine films of titanium oxynitride were deposited using AACVD from precursor solutions of TTIP and TDMAT in toluene at 400 °C, with 25 to 30 min reaction times. Different ratios of TTIP and TDMAT were used for each deposition, although the total amount of precursor in each reaction was maintained at approximately 4×10^{-4} moles. Preliminary results indicated that there was not a direct and proportional relationship between the precursor ratio and the oxygen to nitrogen ratio in the resultant film, as hypothesized in Equation 1. Instead we found that the films were more oxygen rich than would be expected from the precursor ratio. In order to compensate for this, the nine films reported in this work were synthesized with at least 50% TDMAT in the precursor solution, increasing to 100% for the final deposition - as detailed in Table 1.

All nine precursor solutions led to successful film formation, and in the following text the resultant films will be referenced by the molar fraction of TDMAT used in the precursor solution. For example, the film synthesized from a 50:50 ratio of TDMAT and TTIP, with 2×10^{-4} moles of each precursor, will be referred to as the ***50%TDMAT*** film.

XRD Analysis. All of the films were analysed using grazing incident XRD, on a spot 50 mm from the leading edge of the film deposition. This data can be seen in figure 2. The three films made with the highest concentration of the TTIP oxygen precursor, those with TDMAT fractions of 50%, 60% and 64%, visually appeared to be colourless, although there were the presence of iridescent interference fringe colours associated with thin films. The diffraction patterns of these films had Bragg reflections which could be indexed to the *anatase* phase of titanium dioxide - except for the ***50%TDMAT*** film which additionally contained a small peak indicative of some *rutile* phase being present. Rietveld refinement against the diffraction data collected from the ***50%TDMAT*** film indicated that the phase fraction of *rutile* was approximately 15%. Modelling diffraction patterns for the *anatase* phase and refining the lattice parameters against the diffraction data recorded on these three films showed some variation in the *a* and *c* values from sample to sample, as reported in Table 1. However, the variation was less than 0.15% in the *a* parameter, and less than 0.6% in the *c* parameter in comparison to their average, and there was no clear trend within these values. The modelled lattice parameters also all fell within the range reported in the *ICSD* for pure, nitrogen free titanium dioxide. This shows that the nitrogen present within the structure is not significantly affecting the lattice parameters or overall lattice volume. An additional analysis of the effect of particle size on peak broadening was carried out using the Scherrer equation and this gave an estimated particle size for the anatase films of between 30 and 50 nm.

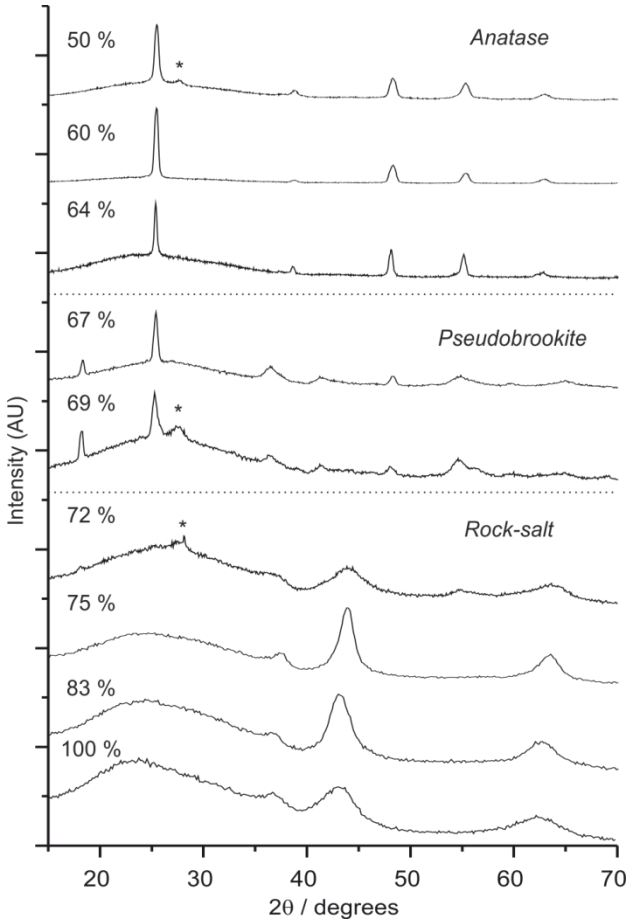

Figure 2. X-ray diffraction patterns of the thin films synthesized from a mixture of TTIP and TDMAT precursor. Patterns are shown descending in order of increasing amounts of TDMAT in the precursor solution, from 50% to 100% TDMAT. The figure is divided into three regions, based on the principle phase observed, and the asterisk (*) identifies the 110 peak of *rutile* structure found in some of the films.

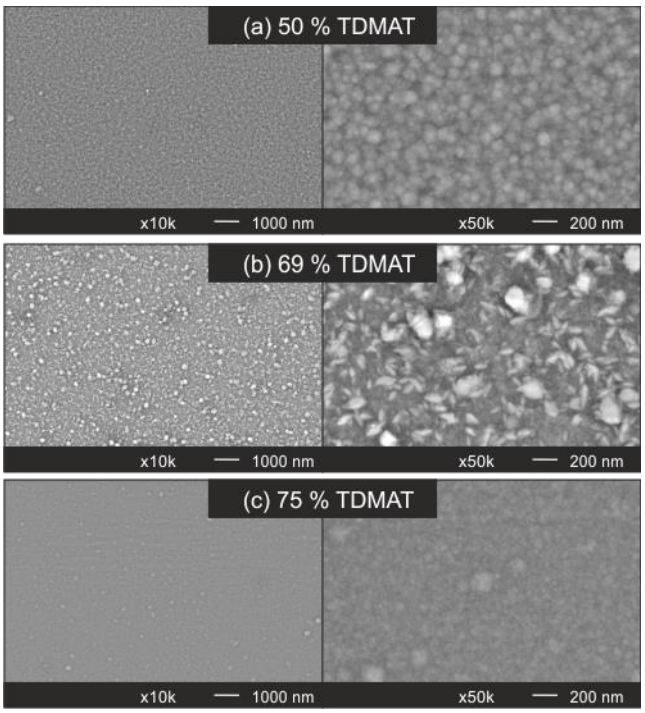

Figure 3. Representative SEM images of the films containing: (a) *anatase* structured titanium oxynitride; (b) *pseudobrookite* structured titanium oxynitride and; (c) *rock-salt* structured titanium oxynitride.

For the films synthesized with next highest amounts of TDMAT in the precursor solution, the ***67%TDMAT*** and ***69%TDMAT*** films, a significant change was observed in the structural composition. These films are blue in colour and contain Bragg peaks that can be indexed to the *pseudobrookite* structure, alongside a small amount of rutile for the ***69%TDMAT*** film. Superficially the pattern of the *pseudobrookite* structure look similar to the *anatase* patterns, however the peak at 18.3° 2θ is indicative of *pseudobrookite*, and combined with the change in colour is strong evidence for the change in phase. Rietveld refinement of this data indicates an overall cell volume for the *pseudobrookite* phase present in the two films of 357.9(1) Å^3 and 360.1(4) Å^3 for ***67%TDMAT*** and ***69%TDMAT*** respectively. Previously reported thin films of the *pseudobrookite* titanium oxynitride with a composition of $Ti_{3-\delta}O_4N$, where $0.19 < \delta < 0.25$, were found to be green in colour with cell volumes of 363.1(1) Å^3 to 364.8(1) Å^3, or brown in colour with $\delta = 0.06$ and a cell volume of 365.5(1) Å^3.[14] The different colour observed in the films reported here, combined with the smaller cell volume indicates that a new composition of *pseudobrookite* titanium oxynitride has been accessed through this route. Scherrer analysis gives particles sizes of 37 and 30 nm respectively.

The four most nitrogen rich precursor mixtures produced films (***72%TDMAT, 75%TDMAT, 83%TDMAT, 100%TDMAT***) with an intense dark-blue colour and X-ray patterns containing

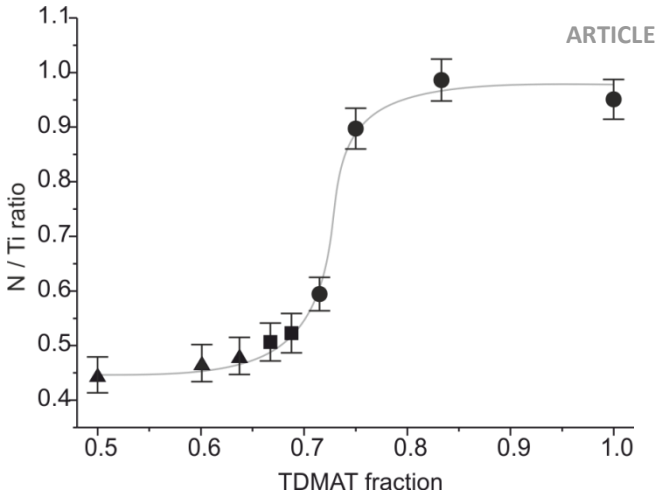

Figure 4. Plot of the nitrogen to titanium atomic ratio determined by WDX as a function of the TDMAT fraction in starting precursor solution. Line is a guide to the eye to indicate the relationship between the two values. Triangles mark samples shown by XRD to be *anatase*, squares *pseudobrookite* and circles *rock-salt*.

broad diffraction peaks, which could be indexed to the *rock-salt* structure of $Ti_xO_yN_z$. As the fraction of TDMAT in the precursor mix increased it led to a shift in the position of the peaks for these samples to lower 2θ angles, which can be modelled as an increase in the lattice parameter from 4.13 Å to 4.20 Å. This is a clear trend of increasing lattice parameter with increasing nitrogen content, as would be expected based on the larger ionic radius of the nitride ion when compared to the oxide ion. However, the *rock-salt* structured films also have a significant loss of crystallinity in comparison to the *anatase* and *pseudobrookite* films, with Scherrer analysis giving relative average crystallite sizes of 6 nm to 10 nm.

Images collected using a field emission SEM can be found in figures S12 and S13. The films identified as having the *anatase* or *rock-salt* structure are smooth, with small densly packed crystallites, giving SEM images with few surface features, and comprised of particles of approximate size of 100-150 nm and 50-100 nm respectively. This supports the much smaller crystallite size observed from analysis of X-ray diffraction peak-width for the *rock-salt* films. The two *pseudobrookite* films have rougher surfaces with variable particle sizes up to 200 nm. Significantly, each group of films, as defined by the principle phase observed from XRD, has a distinct morphology, which are shown in Figure 2 with representative samples of (a) ***50%TDMAT***, (b) ***69%TDMAT*** and (c) ***75%TDMAT***. Side-on SEM, seen in Figure S14, allowed the thickness of each film to be determined. This found a general trend of increasing thickness with increasing amounts of TDMAT used in the precursor mixture, despite the total moles of titanium precursor and reaction time remaining unchanged for each deposition. The *anatase* structured films were between 100-200 nm thick, the *pseudobrookite* titanium oxynitride films were both approximately 300 nm, while the *rock-salt* films were found to be from 380 to 1000 nm thick.

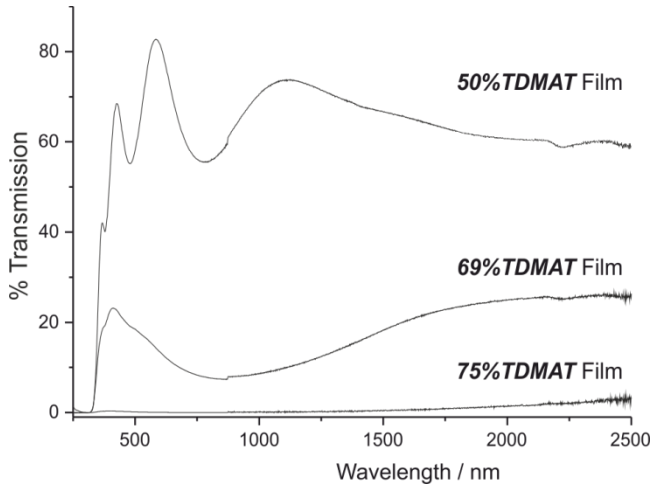

Figure 5. Transmission spectra of the *50%*, *69%* and *75%* films, representative of the patterns observed for the *anatase*, *pseudobrookite*, and *rock-salt* films respectively.

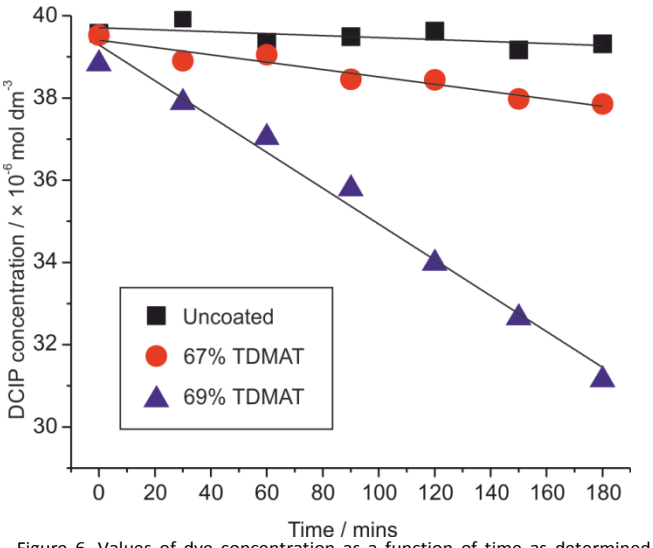

Figure 6. Values of dye concentration as a function of time as determined using visble light spectroscopy, for the photocatalytic tests of uncoated glass and the *67%TDMAT* and *69%TDMAT* samples, over three hours, under 365 nm UV irradiation.

Compositional Analysis. The elemental composition of the samples was investigated using WDX and EDX analysis. The EDX analysis allowed rapid assessment of all of the elements present. In order to achieve sufficient energy to excite the titanium in the sample an acceleration voltage of 10 keV was used, however at this energy the beam penetrated through the film into the substrate for all the samples, causing strong signals which could be assigned to O, Si, Na, Mg and Al - originating from the float glass substrate. This meant that the oxygen content of the films could not be accurately determined, as it was not possible to deconvolute the oxygen present in the film from that in the substrate. However, both titanium and nitrogen were detected and assigned in all films.

WDX analysis was then carried out to more accurately determine the nitrogen and titanium content of each film. The nitrogen per titanium ratio is plotted against the fraction of TDMAT in the precursor mix in Figure 4, and shows the expected overall trend of increasing nitrogen content in the film as the ratio of TDMAT to TTIP in the precursor increases, although this is non-linear. The three colourless films - identified from XRD as being composed principally of the *anatase* phase - have the lowest nitrogen contents, with atomic ratios of 0.44 to 0.48. The WDX confirms that these are nitrogen doped *anatase*, with up to 25% anion site doping by nitrogen, with approximate formulations of $TiO_{1.34}N_{0.44}$, $TiO_{1.31}N_{0.46}$ and $TiO_{1.28}N_{0.48}$ if we assume that titanium must be in its maximum oxidation state, based on the absence of colour in the films.

The *pseudobrookite* structured samples have nitrogen to titanium ratios of 0.50 and 0.52, which are consistent with approximate formulations of $Ti_3O_{3.49}N_{1.51}$, and $Ti_3O_{3.45}N_{1.55}$ assuming full occupation of the cation and anion sites. This gives a fractional titanium oxidation state, of approximately +3.84, consistent with the strong colour of the films.

The most oxygen rich *rock-salt* sample, ***72%TDMAT***, was found to have nitrogen to titanium ratio of 0.59(3), but a small increase in the nitrogen source precursor to ***75%TDMAT*** led to a significant increase in the observed nitrogen content with a nitrogen to titanium ratio of 0.89(4). The final samples of ***83%TDMAT*** and ***100%TDMAT*** had nitrogen to titanium ratios of 0.99(4) and 0.95(4). Making the assumption that there are no cation or anion vacancies within the structure we can estimate the oxygen content and give approximate compositions for these four samples as $TiO_{0.41}N_{0.59}$, $TiO_{0.11}N_{0.89}$, *TiN*, and $TiO_{0.05}N_{0.95}$ respectively.

The compositional analysis from WDX shows that the TDMAT to TTIP ratio can be used to control the composition of the film as anticipated, but the relationship between precursor content and composition is neither direct nor linear, with a sensitivity that varies across the range. For the TDMAT-TTIP system, the precursor mixtures with between 65 and 80% TDMAT provide the greatest sensitivity and allow access to most of the compositional range, as can be seen in figure 4. The reason for the insensitivity at higher or lower precursor ratios remains unclear.

Spectroscopy. Transmission spectra of the films were recorded across the range of 200-2500 nm. Three representative examples of these are shown in Figure 5, one for each of the structure types; remaining data can be found in the Supporting Information. The *anatase* structured films showed high transparency across the visible and near infra-red region, with interference oscillations; the example of the ***50%TDMAT*** film is shown in Figure 5. The spectra of the *pseudobrookite* ***69%TDMAT*** film is also shown, which has a much lower transmission, with an apparent broad absorption centred around 850 nm. The *rock-salt* films represented by the ***75%TDMAT*** film, show almost no transparency across the visible region (less than 10%) although in some cases this rises up to 20% in the IR at 2500 nm, see Figure S9. The three distinct types of spectra reinforce the conclusions regarding the different structures and compositions found by XRD.

Photocatalysis. The photocatalytic ability of the two films containing *pseudobrookite* structured titanium oxynitride were assessed using DCIP dye degradation under both visible light and UV irradiation. For the visible light test an intense 5-sun solar simulator was used, however no degradation of the dye was observed over the 3 hour reaction time, with either the pseudobrookite films or the control. For the UV only test a lower power 4.0 mW cm^{-2} 365 nm light source was used, and under this UV light DCIP reduction was observed with both films, whereas the blank control remained unchanged, as can be seen in Figure 6. Over the three hour experiment dye degradation appeared linear, likely due to saturation of active sites with the dye which is present in large excess, so that 0^{th} order kinetics can be approximated. The ***67%TDMAT*** film had a rate constant of 0.9×10^{-9} $moldm^{-3}min^{-1}cm^{-2}$, while the ***69%TDMAT*** film had a rate constant of 3.6×10^{-9} $moldm^{-3}min^{-1}cm^{-2}$. These values can be compared with a film of titanium dioxide previously measured under the same conditions which had a rate constant of 1.8×10^{-9} $moldm^{-3}min^{-1}cm^{-2}$.[36]

Discussion. The XRD, spectroscopic and WDX data all confirm that AACVD from a mixture of TDMAT and TTIP can be used for the synthesis of titanium oxynitrides, and that the ratio of the titanium-oxygen source precursor and titanium-nitrogen source precursor is then reflected in the composition and structure of the resultant film. The use of mixtures of TTIP and TDMAT with the amide precursor at fractions of up to 65% allows access to nitrogen doped titania, with the *anatase* structure up to a composition of $TiO_{1.28}N_{0.48}$, assuming substitutional doping. For film depositions from precursor solutions with less TTIP, those with 65-80% TDMAT, the film composition appears to be much more sensitive to the precursor ratio, with a slight increase in TDMAT leading to a large increase in the nitrogen incorporated within the film. It is in this precursor mixture range that there is a rapid transfer to the *pseudobrookite* structure, and then *rock-salt* as the principle phase identified within the film.

An additional key finding of our study is the *pseudobrookite* titanium oxynitride with approximate composition $Ti_3O_{3.5}N_{1.5}$, that was blue in colour and had an oxidation state of +3.8. This can be compared to the previously identified green-brown $Ti_{3-\delta}O_4N$ films synthesised by atmospheric pressure CVD, identified with a similar titanium oxidation state, found in the range of +3.74 to +3.96, but with lower nitrogen content. The more nitrogen rich *pseudobrookite* reported here has a smaller unit cell of 358-360 Å³ compared to 362-365 Å³ for the more oxygen rich *pseudobrookite*. This discovery does highlight that a range of anion compositions are possible within the $Ti_{3-\delta}O_{5-x}N_x$ range. These materials are of interest because of the computational prediction of visible light activated photocatalysis in the most nitrogen rich end member, $Ti_3O_3N_2$.[20] Previous work has shown that $Ti_{3-\delta}O_4N$ is a photocatalyst under UV light,[19] and the results presented here show that the more nitrogen rich $Ti_3O_{3.5}N_{1.5}$ is also an active UV light photocatalyst, comparable to titanium dioxide. The possible visible light active $Ti_3O_3N_2$, however, remains elusive.

Conclusions

We have confirmed our hypothesis and shown that through the use of aerosol assisted chemical vapour deposition it is possible to combine two single source precursors to explore a mixed anion ternary phase diagram. We have shown that mixtures of different ratios of titanium isopropoxide and tetrakis(dimethylamido) titanium can be used to deposit a *range of titanium oxynitride structures and compositions. We* have also identified a new composition of *pseudobrookite* titanium oxynitride, which is a UV activated photocatalyst.

The use of precursor solutions of known concentration in this AACVD method allows for more accurate, controlled simultaneous delivery of the two precursors than would be possible in competing techniques. This is a simple method which could be productively applied to other mixed anion phase thin film systems.

Conflicts of interest

There are no conflicts to declare.

Acknowledgements

The authors thank the EPSRC for funding through grant reference EP/K039466/1. We also wish to thank the Leverhulme Trust for funding through RPG-2014-204.

Notes and references

1 F. Oehler and S. G. Ebbinghaus, *Solid State Sci.*, 2016, **54**, 43
2 M.-L. Liu, L.-B. Wu, F.-Q. Huang, L.-D. Chen and I.-W. Chen*, J. Appl. Phys.*, 2007, **102**, 116108
3 S. Ghannadzadeh, J. D. Wright, F. R. Foronda, S. J. Blundell, S. J. Clarke and P. A. Goddard, *Physical Review B*, 2014, 89
4 K. L. Choy, *Prog. Mater. Sci.*, 2003, **48**, 57
5 C. E. Knapp and C. J. Carmalt, *Chem. Soc. Rev.,* 2016, **45**, 1036
6 M. J. Powell and C. J. Carmalt, *Chem - A Euro J., 2*017, **23**, 15543
7 P. Marchand, I. A. Hassan, I. P. Parkin, C. J. Carmalt, *Dalton Trans.*, 2013, **42**, 9406
8 G. Hyett, M. A. Green and I. P. Parkin, *Chem. Vap. Deposition*, 2008, **14**, 309
9 N. D. Boscher, C. J. Carmalt, G. Hyett, A. G. Prieto, Q. A. Pankhurst and I. P. Parkin, *J. Mater. Chem.*, 2008, **18**, 1667
10 E. S. Peters, C. J. Carmalt, I. P. Parkin and D. A. Tocher, Eur. *J. Inorg. Chem.*, 2005, 4179
11 C. Edusi, G. Hyett, G. Sankar and I. P. Parkin, *Chem. Vap. Deposition*, 2011, **17**, 30
12 J. N. Musher and R. G. Gordon, *J. Mater. Res.*, 1996, **11**, 989
13 F. Maury and F. D. Duminica, *Surf. Coat. Technol.*, 2010, **205**, 1287
14 G. Hyett, M. A. Green and I. P. Parkin, *J. Am. Chem. Soc.*, 2007, **129**, 15541
15 A. Mills and S. LeHunte, *J. Photochem. Photobiol.*, A, 1997, **108**, 1
16 C. W. H. Dunnill, Z. A. Aiken, J. Pratten, M. Wilson, D. J. Morgan and I. P. Parkin, *J. Photochem. Photobiol.*, A, 2009, **207**, 244
17 R. Asahi, T. Morikawa, T. Ohwaki, K. Aoki and Y. Taga, *Science*, 2001, **293**, 269
18 C. W. Dunnill and I. P. Parkin, *Dalton Trans.*, 2011, **40**, 1635

19 G. Hyett, M. A. Green and I. P. Parkin, J. Photochem. Photobiol., A, 2009, **203**, 199
20 Y. Wu, P. Lazic, G. Hautier, K. Persson and G. Ceder, *Energy & Env. Sci.*, 2013, **6**, 157
21 Y. F. Zheng, K. Kikuchi, M. Yamasaki, K. Sonoi and K. Uehara, *Appl. Opt.*, 1997, **36**, 6335
22 C. W. Dunnill and I. P. Parkin, *Chem. Vap. Deposition*, 2009, **15**, 171
23 M. J. Powell, R. G. Palgrave, C. W. Dunnill and I. P. Parkin, *Thin Solid Films*, 2014, **562**, 223
24 S. Andersson and A. Magneli, *Naturwissenschaften*, 1956, **43**, 495
25 G. Shirane, S. J. Pickart and R. Newnham, *J. Phys. Chem. Solids*, 1960, **13**, 166
26 M. G. Kostenko, A. V. Lukoyanov, V. P. Zhukov and A. A. Rempel, *J. Solid State Chem.*, 2013, **204**, 146
27 M. E. Straumanis, *J. Appl. Phys.*, 1959, **30**, 1965.
28 S. Andersson, B. Collen, U. Kuylenstierna and A. Magneli, *Acta Chem. Scand.*, 1957, **11**, 1641
29 A. N. Christensen, A. Alamo and J. P. Landesman, *Acta Crystallographica Section C-Crystal Structure Communications*, 1985, **41**, 1009
30 B. Holmberg, *Acta Chem. Scand.*, 1962, **16**, 1255
31 C. Norlund, *Acta Chem. Scand.*, 1978, **32**, 89
32 C. Norlund, *Acta Chem. Scand.*, 1975, **29**, 563
33 R. D. Shannon, *Acta Crystallographica Section A*, 1976, **32**, 751
34 N. Serpone, *The Journal of Physical Chemistry B*, 2006, 110, 24287-24293.
35 A. Mills and M. McGrady, *J. Photochem. Photobiol., A,* 2008, **193**, 228-236.
36 N. J. Platt, K. M. Kaye, G. J. Limburn, S. D. Cosham, A. N. Kulak, R. G. Palgrave and G. Hyett, *Dalton Trans.*, 2017, **46**, 1975